https://doi.org/10.5194/cp-2020-107
Preprint. Discussion started: 25 August 2020

Climate of the Past Discussions

Cryogenic cave carbonates in the Dolomites (Northern Italy): insights into Younger Dryas cooling and seasonal precipitation

Gabriella Koltai[1], Christoph Spötl[1], Hai Cheng[2, 3, 4]

[1] Institute of Geology, University of Innsbruck, Innrain 52d, 6020 Innsbruck, Austria
[2] Institute of Global Environmental Change, Xi'an Jiaotong University, Xi'an, China
[3] State Key Laboratory of Loess and Quaternary Geology, Institute of Earth Environment, Chinese Academy of Sciences, Xi'an, China
[4] Department of Earth Sciences, University of Minnesota, Minneapolis, MN, USA

Correspondence to: Gabriella Koltai (gabriella.koltai@uibk.ac.at)

Abstract. In the European Alps, the Younger Dryas (YD) was characterized by the last major glacier advance with equilibrium line altitudes being ~220 to 290 m lower than during the Little Ice Age and also by the development of rock glaciers. Dating of these geomorphic features, however, is associated with substantial uncertainties leading to considerable ambiguities on the internal structure of this stadial, the most intensively studied one of the last glacial period. Here we provide robust physical evidence based on precise ^{230}Th-dated cryogenic cave carbonates (CCC) coupled with thermal modelling indicating that early YD winters were only moderately cold in the Southern Alps, challenging the commonly held view of extreme YD seasonality. Our data argue for a negative temperature anomaly of ≤ 3°C in mean annual air temperature at the Allerød-YD transition in a mountain cave (Cioccherloch, 2274 m a.s.l.) in the Dolomites of northern Italy. Our data suggest that autumns and early winters in the early part of the YD were relatively snow-rich, resulting in a stable winter snow cover. The latter insulated the shallow subsurface in winter and allowed the cave interior to remain close to the freezing point (0°C) year-round, promoting CCC formation. The main phase of CCCs precipitation at ~12.2 ka BP coincides with the mid-YD transition recorded in other archives across Europe. Based on thermal modelling we propose that CCC formation at ~12.2 ka BP was most likely associated with a slight warming of approximately +1°C in conjunction with drier autumns and early winters in the second half of the YD. These changes triggered CCC formation in this alpine cave as well as ice glacier retreat and rock glacier expansion in the Alps.

1 Introduction

The last glacial period in the Northern Hemisphere (from 119 to 11.7 thousand years (ka) BP; Rasmussen et al., 2014) was characterized by abrupt climate shifts from cold and commonly arid stadials to mild and more humid interstadials. The youngest of these stadials is known as the Younger Dryas (YD or Greenland Stadial (GS) 1, ~12.8 to 11.7 ka BP; Rasmussen et al., 2014) and was a period when Northern Hemisphere temperatures returned to near-glacial levels, interrupting the last Termination.

https://doi.org/10.5194/cp-2020-107
Preprint. Discussion started: 25 August 2020


Climate of the Past Discussions

The YD is among the most extensively studied periods in the late Quaternary due to the availability of high-resolution palaeoclimate records such as ice, marine and lacustrine sediment cores. Still, the forcing mechanism(s) for this cold episode remain debated (Alley, 2000; Baldini et al., 2018; Brauer et al., 2008; Broecker et al., 2010; Renssen et al., 2015). The most widely accepted model invokes a near-shutdown of the Atlantic Meridional Overturning Circulation (AMOC) as a result of catastrophic meltwater injection into the North Atlantic Ocean (e.g. Broecker et al., 1989), and the concomitant large-scale reorganization of the westerlies due to extensive winter sea ice formation (e.g. Bakke et al., 2009; Brauer et al., 2008). The resulting southward displacement of the polar front and the westerlies led to cold, almost Siberian-like conditions in N and NW Europe during prolonged winters (e.g., Broecker, 2006). In a recent study using a European-wide compilation of plant indicator species Schenk et al. (2018), however, suggested that YD summers remained relatively warm despite the AMOC shutdown with temperature decreases of 4.3ºC in NW Europe and 0.3ºC in eastern Europe relative to the preceding Bølling-Allerød interstadial (Greenland Interstadial (GI) 1). Using climate model simulations, Schenk et al. (2018) attributed relatively warm summers to atmospheric blocking induced by the Fennoscandian Ice Sheet preventing the penetration of cold westerly air masses entering Europe during the short summers. In contrast, blocking was almost absent during YD winters (Renssen et al., 1996). Overall, proxy data suggest that the YD climate was dominated by high seasonality and continentality across Europe with large meridional summer temperature gradients (e.g. Heiri et al., 2014a). Changes in winter climate were likely disproportionally larger (e.g. Broecker, 2006), but quantitative understanding of the YD climate remains heavily biased towards the summer given the scarcity of winter proxy data.

Speleothem-based palaeotemperature reconstructions from the Jura Mountains in northern Switzerland suggest a large drop of the mean annual air temperature (MAAT) of up to -10°C during the YD (Affolter et al., 2019; Ghadiri et al., 2018), while preliminary results of a similar study from a cave in western Austria suggest a much smaller difference (5.5°C) (Luetscher et al., 2016). Rock glacier records from the SE Swiss Alps argue for an even smaller cooling of only up to 3-4°C (Frauenfelder et al., 2001).

More recently, evidence for a time-transgressive climate shift mid-way through the YD has been reported from lacustrine sediments (e.g. Bakke et al., 2009; Brauer et al., 2008; Schlolaut et al., 2017), speleothems (Baldini et al., 2015; Bartolomé et al., 2015; Rossi et al., 2018) and marine sediments in Europe (Naughton et al., 2019). This climate shift has been attributed to a gradual northward movement of the polar front driven by the resumption of the AMOC and concomitant sea-ice retreat in the North Atlantic. The earliest indication of a climate shift during the mid-YD is recorded by a stalagmite from the Pyrenees, showing a gradual transition from dry to wet conditions starting at 12.45 ka BP (Bartolomé et al., 2015). It took about three hundred years for this shift to propagate to central and finally to northern Europe, where it is documented as a rapid change in certain proxy properties (Bakke et al., 2009; Lane et al., 2013). While many records from SW (Baldini et al., 2015; Bartolomé et al., 2015; Naughton et al., 2019; Rossi et al., 2018) and N Europe indicate that the first half of the YD was colder and drier than the second one, biomarker data from lacustrine sediments of the Gemündener Maar in W Germany suggest the opposite trend (Hepp et al., 2019).

https://doi.org/10.5194/cp-2020-107
Preprint. Discussion started: 25 August 2020


Climate of the Past Discussions

In the Alps, climate information about the YD has been traditionally derived from studies of lake sediments (e.g. Grafenstein et al., 1999; Heiri et al., 2014; Lauterbach et al., 2011) and glacier reconstructions (e.g. Ivy-Ochs et al., 2009; Kerschner et al., 2000; Kerschner and Ivy-Ochs, 2008; Moran et al., 2016), complemented by a few cave records (Luetscher et al., 2016; Wurth et al., 2004). Studies on the internal structure of the YD, however, are rare and compromised by poor dating resolution, limiting our understanding of the mechanism(s) of the proposed mid-YD climate shift. Alpine paleoglacier records suggest an early YD glacier maximum between about 13.5 and 12.0 ka BP attributed to a combination of low temperatures and enhanced precipitation differences between the northern, central and southern part of the Alps (Kerschner et al., 2016; Kerschner and Ivy-Ochs, 2008). Equilibrium line altitude reconstructions show that the inner zone of the Alps received ~20-30% less precipitation than today, mostly due to a decrease in winter precipitation, while annual precipitation in the Southern Alps was probably similar to modern values (Kerschner et al., 2016). Paleoglaciers from the Southern Alps show evidence of a double response, whereby the outermost and innermost moraines stabilized at ~12.3±0.7 ka and before 11.2±0.8 ka BP, respectively (Baroni et al., 2017; Ivy-Ochs et al., 2009).

In this study we focus on the Dolomites in the Southern Alps and provide seasonally resolved insights into the climate of the YD from cave sediments anchored by a precise ^{230}Th chronology. Rather than examining stalagmites commonly used in speleothem-based palaeoclimate research, we utilize a rather novel speleothem variety which provides a uniquely robust temperature control: coarsely crystalline cryogenic cave carbonate (CCC for short). The leading genetic model envisages CCC formation under degrading permafrost conditions (e.g., Žák et al., 2018). Water ingresses into the cave when the seasonally thawing active layer of permafrost intersects the ceiling of the cave chamber, while most of the chamber is still within the permafrost, resulting in cave ice formation. Further climate warming leads to progressive degradation of permafrost and the cave air temperature slowly rises to 0°C. Drip water creates meltwater pools in the cave ice bodies that freeze slowly triggering the precipitation of CCC. Regardless of the details of this model, the key point is that CCC form within perennial cave ice at temperatures very close to 0°C (Žák et al., 2018).

Using a strategically selected high-alpine cave whose paleothermal regime is assessed using heat-flow modelling, we use CCC data to argue against strong winter cooling during the early YD, provide evidence of a maximum of 1-2°C warming at the mid-YD transition, and show that autumns and winters became drier in the second half of the YD.

2 Study site

Cioccherloch is a single-entrance cave opening at 2245 m a.s.l. on the karst plateau of the Sennes region in the Dolomites. Given that the early YD polar front was supposedly located south of the main crest of the Alps (Lane et al., 2013), this site in the Southern Alps is ideal to trace the northward migration of the polar front (Fig. 1). The cave has approximately 250 m of passages. The entrance shaft is 20 m deep and intersects a subhorizontal cave level. A firn and ice cone is present at the bottom of this shaft fed by winter snow sliding down the shaft. Separated by a narrow squeeze which was excavated by cavers, a separate branch of the cave 60 m long and up to 10 m high descends from this cave level to approximately 55 m below the

https://doi.org/10.5194/cp-2020-107
Preprint. Discussion started: 25 August 2020


Climate of the Past Discussions

surface. Near the lower end of this gallery CCC were discovered for the first time in the Dolomites (Fig. 1). The air temperature at the CCC site monitored over a 1-year-period averages 2.5°C with minimum values (2.2°C) in January to March and maximum values (2.7°C) in November. These data show that the cave chamber is in thermal equilibrium with the outside MAAT at this elevation, obtained from nearby weather stations at Rossalm (2340 m a.s.l.) and Piz la Ila (2050 m a.s.l.) located less than 10 km from the study site. The mean air temperature is 2.2°C and 3.3°C at Rossalm and Piz la Ila, respectively (2015-2018; data source: Hydrographisches Amt, Autonome Provinz Bozen – Südtirol). The majority of snowfall in the Dolomites occurs from January to April with average snow heights of 4.2 and 3.4 m at Rossalm (2012-2019) and Piz la Ila (1999-2014), respectively. Autumn to early winter (September to December) snowfall amounts to an average of 1.0 and 0.8 m at the two weather stations.

3 Methods

3.1 Field work

CCC occurrences were mapped and samples were collected from five distinct heaps labelled A to E (Suppl. Fig. 1). In addition, small in-situ stalagmites were taken from the same chamber. Cave air temperature was recorded on an hourly basis using a Hobo Temp Pro v2 logger (Onset) between August 2016 and July 2017.

3.2 Morphological characterization

CCC samples were cleaned in an ultrasonic bath prior to documentation and laboratory analyses. Individual morphologies were examined using a Keyence VHX-6000 digital microscope.

3.3 Stable isotope analyses

CCCs samples were analyzed for their stable oxygen and carbon isotope composition using isotope ratio mass spectrometry (Spötl and Vennemann, 2003). In addition, two larger CCC particles were cut in half and micromilled at 0.1 to 0.3 mm resolution. The results are reported relative to the VPDB standard with a long-term precision better than ±0.08‰ (1σ) for both $\delta^{13}C$ and $\delta^{18}O$.

3.4 ^{230}Th dating

Seventeen individual CCC particles were selected for ^{230}Th dating. 15-20 mg of calcite was drilled using a handheld drill from 15 crystals in a laminar flow hood. Two skeletal CCC crystals were analyzed as a whole as they were too small for aliquots to be drilled from them. Growth layers of a stalagmite (Cioc1) collected next to the CCC spots were drilled at three discrete horizons (2, 24 and 50 mm from the top) and prepared for analyses.

https://doi.org/10.5194/cp-2020-107
Preprint. Discussion started: 25 August 2020


Climate of the Past Discussions

Ages were determined by measuring U and Th isotope ratios on a multi-collector inductively coupled mass spectrometer after their chemical separation following Edwards et al. (1987) and Cheng et al. (2013). Analyses were performed at Xian Jiaotong University (China). 2σ uncertainties for U and Th isotopic measurements include corrections for blanks, multiplier dark noise, abundance sensitivity, and contents of the same nuclides in the spike solution. Decay constants for ^{230}Th and ^{234}U were reported by Cheng et al. (2013). Corrected ^{230}Th ages assume an initial ^{230}Th/^{232}Th atomic ratio of (4.4 ±2.2) ×10^{-6} and ^{232}Th/^{238}U value of 3.8 as the value for material at secular equilibrium with the bulk earth. Final ages are given in years BP (before 1950 AD).

3.5 Thermal modelling

Heat conduction from the surface to 70 m depths was modelled using a 1d heat-flow model (https://zenodo.org/record/3982221). This model considers conductive heat transfer only and solves the heat equation utilizing finite differences as space discretizations alongside a forward Euler time-stepping scheme, stabilized with a diffusion-type Courant–Friedrichs–Lewy condition. The relationship between heat flow Q, thermal conductivity c, and geothermal gradient dT/dz is given by Eq. (1):

$$Q = c \times dT/dz \quad (1)$$

The model assumes a homogenous host rock with no internal heat generation. Thermal diffusivity of the limestone was set to 1.2 x 10^{-6} m^2/s (Hanley et al., 1978) to account for some air-filled porosity. The ground heat flux (dT/dz) was set to 0, to account for the presence of the shaft in the entrance zone of the cave, allowing exchange with the ambient air in this upper part of the cave suppressing the minor effect of the geothermal heat flux. This assumption is supported by the agreement between the temperature at the end of the CCC-bearing cave gallery and the ambient MAAT. Modeling results are shown as MAAT against depth below the surface.

4 Results

4.1 CCC morphology

CCC occur as loose crystals and crystal aggregates in small heaps on and partly underneath five breakdown blocks (Suppl. Fig. 1). Individual crystals and aggregates thereof come in a variety of shapes and sizes, the largest reaching 1.4 cm in length. Morphologies include amber-colored crystals and crystal aggregates of rhombic, raft, beak-like and split crystal habits (Suppl. Fig. 1). Split and beak-like crystals are most abundant (heaps A, B, and D). Translucent skeletal crystals are rarely present in heaps B and D, but are dominant in C and E.

4.2 Stable isotope composition

CCC show high $\delta^{13}C$ values varying from 1.3 to 5.4 ‰ and low $\delta^{18}O$ values ranging from -21.8 to -10.1‰ (Fig. 2, Suppl. Table 1). These values fall within the compositional range characteristic of CCC (Žák et al., 2018 and references therein),

https://doi.org/10.5194/cp-2020-107
Preprint. Discussion started: 25 August 2020


Climate of the Past Discussions

confirming their precipitation in slowly freezing of pockets of water enclosed in cave ice. A beak-like crystal, 4.5 mm in diameter, revealed ≤1.3‰ and ≤1.2‰ intra-crystalline variability in $\delta^{13}C$ and $\delta^{18}O$, respectively, while a 5 mm large rhombohedral crystal shows ≤0.4‰ and ≤0.2‰, respectively. Holocene stalagmites from the same chamber exhibit distinctly different stable isotope values with $\delta^{13}C$ and $\delta^{18}O$ values ranging from -7.6 to -2.0‰ and from -9.1 to -7.4‰, respectively (Fig. 2).

4.3 ^{230}Th dating

The ^{238}U concentration of CCC samples varies from 0.8 to 2.2 ppm (Table 1). Four samples yielded $^{230}Th/^{232}Th$ atomic ratios less than 100×10^{-6}, indicating significant detrital contamination (Table 1) and the corresponding ages were excluded from the discussion. The 2σ precision of the remaining 13 ages ranges from 0.4 to 2.7%.

All CCC ages fall within the YD (as defined by Rasmussen et al., 2014), whereby individual ages show a spread from 12.61 ±0.22 to 12.08 ±0.19 ka BP. Although most of the ages overlap within their 2σ errors, some ^{230}Th ages suggest that CCC formation commenced at the beginning of the YD (i.e. 12.61 ±0.22 ka BP). On the other hand, the error-weighted mean of all ages yielded 12.19 ±0.06 ka BP and 90% percent of ^{230}Th dates cluster at ~12.2 ka BP. There is no systematic age difference between samples from individual heaps nor between different CCC morphologies.

In contrast to CCCs, the ^{238}U concentration of stalagmite Cioc1 is much lower (~0.5 ppm). $^{230}Th/^{232}Th$ atomic ratios vary between 34×10^{-6} and 1570×10^{-6} (Table 1). The resulting ^{230}Th ages demonstrate that stalagmite growth commenced during the Late Glacial at 14.98 ±0.14 ka BP. Petrographic analysis provides strong evidence for a growth interruption after which calcite deposition re-started in the mid-Holocene at 5.88 ±0.15 ka BP and continued until 1.32 ±0.27 BP ka.

4.4 Thermal modelling

We performed a series of model runs covering possible climate scenarios for the YD (Table 2) to explore the relationship between atmospheric temperature changes and the temperature 50 m below the surface at this high-elevation site. We define the thermal boundary conditions for CCC formation as -1 to 0°C ("CCC window" - see discussion) whereby the likelihood of CCC formation is highest between -0.5 and 0°C.

Paleotemperature estimates used in these computations are based on regional annual and summer air temperature reconstructions. Three of the models (scenarios 2c, 2e and 3c) also consider the insolating effect of a winter snow cover, expressed as ΔTs, i.e. the buffering of the winter temperature at the ground surface by the snow cover (following Zhang, 2005; Table 2).

4.4.1 Scenario 1 – Allerød interstadial

In this scenario we simulated an interstadial, similar to the 1000 year-long Allerød preceding the YD, in order to precondition the thermal regime of the subsurface (Table 2). We assumed that no permafrost was present at the site at the start of the

https://doi.org/10.5194/cp-2020-107
Preprint. Discussion started: 25 August 2020


Climate of the Past Discussions

interstadial (hence a ground temperature of 1°C at the surface). The experiment was forced with a MAAT 2°C lower than present day (i.e., $\Delta MAAT_{Modern\text{-}Allerød}$=-2°C) consistent with regional proxy data (e.g., Ilyashuk et al., 2009). After 1000 years a temperature of 0.5°C is reached at 50 m depth (Suppl. Fig. 2). The model output was used as the initial setup for all scenario 2 models.

4.4.2 Scenario 2 – Stadial conditions during the early YD

In the next five experiments (2a – 2e) we explored the timing of perennial cave ice development and tested whether water pockets in cave ice could have experienced slow freezing during an early YD characterized by cold stadial conditions. As the mid-YD transition was determined at 12,240 ± 40 varve years BP at Meerfelder Maar, Germany (Lane et al., 2013), scenario 2 models were run for 610 years (i.e. from 12.85 to 12.24 ka BP).

Scenario 2a was forced with a $\Delta MAAT_{Modern\text{-}early\ YD}$ of -9°C (i.e. $\Delta MAAT_{Allerød\text{-}early\ YD}$ = -7°C; -20°C in January; Table 2), consistent with speleothem-based paleotemperatures from northern Switzerland (Affolter et al., 2019; Ghadiri et al., 2018). The results show that the atmospheric cooling rapidly propagates into the subsurface resulting in the development of permafrost down to 50 m depth in less than 50 years (Fig. 3a, Suppl. Fig. 3a).

In scenario 2b we applied a less dramatic atmospheric cooling characterized by $\Delta MAAT_{Modern\text{-}early\ YD}$ of -5°C (i.e. $\Delta MAAT_{Allerød\text{-}early\ YD}$ = -3°C; -13°C in January; Table 2). This cooling amplitude has been suggested by stalagmite fluid inclusion data from western Austria (Luetscher et al., 2016). Modelling results show that the cave 50 m below the surface cools to -1°C in about 100 years. Further cooling would lead to -2.0°C about 100 years later (Fig. 3b, Suppl. Fig. 3b).

The third stadial experiment (2c) investigates the influence of an autumn/early winter snow cover (Table 2) insulating the ground from cold air during winter, assuming a buffering of the winter temperatures by the snow cover of 5°C (i.e. ΔT of 5°C). The presence of a snow pack delays the cooling of the ground and results in temperatures at 50 m depth between 0.5 and -1°C within 150 years from the start of the atmospheric cooling (Fig. 3c, Suppl. Fig. 3c).

Scenarios 2d and 2e consider an even smaller drop in MAAT ($\Delta MAAT_{Modern\text{-}early\ YD}$ = -4.5°C i.e. -12°C in January; Table 2), as suggested by rock glacier records from the Southern Alps (Frauenfelder et al., 2001). With no winter snow cover (2d) the temperature at the CCC site reaches -0.5°C after ~60 years and drops below -1°C (i.e. it leaves the "CCC window") after 100 years (Fig. 3d, Suppl. Fig. 3d). On the other hand, if snow insolates the ground in winter and buffers the winter cold by 4.7 °C (i.e. ΔT of 4.7°C; Table 2), temperatures at 50 m depth stay above -0.8°C for an extended period of time (Fig. 3e, Suppl. Fig. 3e).

4.4.3 Scenario 3 – Stadial conditions during the late YD

Three experiments were designed to explore the impact of climate change at the mid-YD transition, starting at 12.24 ka BP (Lane et al., 2013), on the subsurface thermal regime at this high-alpine site (Table 2). In the first experiment (3a) we examined how permafrost conditions would change with increasing aridity in autumn compared to the early YD (2e). As the insulating effect of the winter snowpack is reduced, the depth zone of the CCC site experiences rapid cooling and approaches -1.8°C

https://doi.org/10.5194/cp-2020-107
Preprint. Discussion started: 25 August 2020


Climate of the Past Discussions

after 100 years, leading to permafrost development, inconsistent with stable conditions near 0°C required for CCC formation (Fig. 4a, Suppl. Fig. 4a)

We applied a +1°C change in MAAT represented by a 2°C rise in January temperatures with (3c) and without (3b) snow cover (Table 2). We kept the climate warming at 1°C (i.e. $\Delta MAAT_{Allerød\text{-}late\ YD}$= -2°C), because a larger warming would result in a climate similar to the preceding Allerød. The results of scenario 3b demonstrate that even though winters become slightly less cold, the subsurface at 50 m depth would nevertheless cool from -1.3°C to -1.5°C due to the lack of a winter snow cover. This scenario is not compatible with CCC formation as it leads to permafrost aggradation (Fig. 4b, Suppl. Fig. 4b). In contrast, even the presence of a moderate snow cover (3c) would allow the subsurface at 50 m depth to slowly warm to -1°C after 75 years of the start of the atmospheric warming (Fig. 4c, Suppl. Fig. 4c), creating favorable conditions for slow freezing of liquid water pockets in the ice introduced by dripping water.

5. Discussion

5.1 0°C conditions in the shallow subsurface

CCCs form in slowly freezing water pockets enclosed in cave ice when the cave interior temperature is very close to the 0°C isotherm (e.g., Žák et al., 2018). Although the deposition of CCCs in many cases mark climate transitions (e.g., Richter and Reichelmann, 2008; Spötl and Cheng, 2014; Žák et al., 2012), the large size of some CCCs (up to 50 mm in caves elsewhere, unpublished data from our group) and ^{230}Th ages from their central and rim areas (unpublished data from our group) argue for very stable cave microclimate conditions for at least several years (e.g., Žák et al., 2018).

CCCs (Table 2) provide unequivocal evidence that perennial ice was present in the lower descending gallery of Cioccherloch during the first part of the YD. As the majority of ^{230}Th ages overlap within their 2σ errors, it is not possible to determine whether CCC formation took place continuously for 400-600 years or if they represent two different generations clustering at ~12.6 and ~12.2 ka BP (Fig. 5). The diversity of morphologies and the occurrence of discrete spots nevertheless supports the latter, indicating the presence of several CCC-forming water pockets/pools. Overall, CCCs in Cioccherloch record interior cave air temperatures very close to 0°C from ~12.6 to ~12.2 ka BP, initiating progressive freezing of meltwater pockets in perennial ice which were created by drip water.

The air temperature in the homothermic zone of caves is in equilibrium with the MAAT of the outside atmosphere. Ice-bearing caves, however, commonly represent an exception to this rule (e.g., Perșoiu, 2018 and references therein.). Due to its descending geometry lacking a lower entrance, Cioccherloch is a cold trap, as evidenced by the snow and ice cone at the base of the entrance shaft. This negative thermal anomaly, however, is restricted to the upper cave level close to the snow cone. Today, the descending gallery with the CCC occurrences is thermally isolated from this upper level due to the narrow connection, as shown by stable cave air temperatures consistent with the ambient mean MAAT (2.4°C). Prior to cave exploration in the 1980s and 1990s, this squeeze was partly closed by rubble. Therefore, we presume that this descending gallery has been thermally decoupled from the upper cave level in the past and remained in thermal equilibrium with the

https://doi.org/10.5194/cp-2020-107
Preprint. Discussion started: 25 August 2020

ambient atmosphere. As a result, CCCs in the lower gallery record changes in the thermal state of the subsurface in relation to atmospheric temperature changes. Given the lack of ventilated shafts connecting this gallery to the surface, we argue that heat exchange between the latter and the gallery occurred primarily via conduction. Additional heat transfer may involve drip water influx and minor air advection via possible small-scale fissures in the ceiling. These processes are difficult to quantify for any time in the past and no attempts were made to include them in the thermal model. Qualitatively, both processes would increase the rate of temperature change in this gallery as a response to atmospheric change above the cave. By considering heat conduction only, our simulations yield quantitative constraints on the maximum duration of temperature change propagated into the shallow subsurface.

The formation of CCCs near the lower end of the descending gallery requires the 0°C isotherm to be located at 50 m below the ground surface at 2274 m a.s.l. in the Dolomites during the YD. On the other hand, stalagmite Cioc1 from the same gallery provides strong evidence that subsurface conditions were favorable for speleothem growth during the Bølling-Allerød interstadial. In other words, during this interstadial this gallery was free of ice and the cave air temperature was above 0°C. During the early YD, atmospheric cooling led to the aggradation of cave ice. Probably during the warm YD summers (from ~12.6 to ~12.2 ka BP) drip water from torrential rains and/or snowmelt created meltwater pools that subsequently underwent slow freezing cycles, requiring a cave air temperature in this gallery ~2-3°C (i.e. 2.5 ± 0.5°C) lower than today.

CCC deposition in caves is traditionally attributed to near-surface permafrost degradation in response to atmospheric warming (e.g. Žák et al., 2018 and references therein). However, stalagmite growth indicates that CCC formation in Cioccerloch cave does not represent a delayed response of the Bølling-Allerød interstadial warming. Instead our data suggest that CCCs in Cioccherloch may formed during transitions into cold periods. Therefore, we hypothesize that analogous to climate warmings possible "CCC windows" opened during the transition into stadials and remained open for a variably long period of time depending on the local thermal conditions of the subsurface.

5.2 Magnitude of YD cooling

CCCs dated to the first and second half of the YD suggest conditions very close to 0°C for an extended period of time during this stadial. Our thermal model shows the CCC formation starting at 12.6±0.2 ka BP at this sensitive mountain site can only be reconciled by evoking a moderate atmospheric cooling at the Allerød-YD transition of -4.5 to -5°C relative to today (Fig. 5). Without a winter snow cover (scenarios 2b and 2d) the "CCC window" would open too early and close quickly afterwards, inconsistent with the CCC ages (Fig. 5). Scenario 2c and 2e shows that if the YD climate was characterized by a -5 to -4.5°C drop in MAAT relative today (i.e. $\Delta MAAT_{Allerød\text{-}YD}$= -3 to -2.5°C), a thick and stable snow cover during winter is needed to prevent the cave from freezing, effectively shielding the ground from the cold stadial winters (Zhang, 2005). Scenario 2e including provides the best fit with the CCC data giving rise to a 400 year-long period characterized by a very slow cooling of the subsurface with cave air temperatures near -0.8°C.

Our data do not support the notion of a very cold YD ($\Delta MAAT_{Modern\text{-}YD}$ = -9 to -10°C; scenario 2a) as suggested by speleothem data from low-lying caves in northern Switzerland (Affolter et al., 2019; Ghadiri et al., 2018). Such a drastic lowering of the

https://doi.org/10.5194/cp-2020-107
Preprint. Discussion started: 25 August 2020


Climate of the Past Discussions

MAAT would freeze Cioccherloch rapidly even if a thin winter snowpack was present, and would result in rather abrupt development and deepening of permafrost, preventing CCC formation (Fig. 7). Such a stark cooling would in fact lead to climate conditions similar to the Last Glacial Maximum (LGM), for which noble gas data from groundwater studies around the Alps suggest 7-10°C lower temperature compared to the Holocene (e.g., Šafanda and Rajver, 2001; Stute and Deak, 1989; Varsányi et al., 2011) and which would inevitably lead to the build-up of glaciers at this elevation in the Dolomites.

Our data, however, are consistent with observations from rock glaciers (Frauenfelder et al., 2001) and lake sediments in the Swiss Alps (Von Grafenstein et al., 2000) suggesting a moderate cooling at the Allerød-YD transition. A fluid inclusion-based paleotemperature reconstruction using stalagmites from Bärenhöhle in western Austria also indicates a maximum temperature drop of about 5.5°C, supporting our interpretation (Luetscher et al., 2016).

5.3 Increased seasonality in the early YD

CCCs provide a uniquely robust control on cave air temperatures and consequently on the MAAT. Our data argue for a ≤3°C drop in MAAT at the Allerød-YD transition, but provide no direct information on the seasonal cycle of ambient atmospheric temperatures. A recent multi-proxy-model comparison by Schenk et al. (2018) suggests persistently warm summers during the YD with a median regional cooling of 3°C and 0.3°C over NW- and E-Europe, respectively, compared to Bølling-Allerød summers. These authors also argue that previous studies using chironomids overestimated the YD cooling signal. A similar amplitude of change is suggested for July air temperatures by lake records from the Western Alps. Pollen and cladocera-inferred temperature reconstructions indicate a summer cooling of 2-4°C at the Allerød-YD transition at Gerzensee (Swiss Plateau, e.g., Lotter et al., 2000), consistent with a 3.5°C drop in July air temperatures reported from Maloja Pass in eastern Switzerland (Oberli et al., 2009). We therefore consider 0.3° and 4°C as minimum and maximum estimates of YD summer cooling, respectively, relative to the Bølling-Allerød. As our CCC data in conjunction with thermal modelling constrain the drop in MAAT at the Allerød-YD-transition to ≤3°C, we find that if YD summers were indeed 0.3 to 4°C colder than in the Allerød, early YD winters at 2270 m a.s.l. were no colder than -13.7°C (mean January temperature). This argues for an enhanced seasonality in the Dolomites, whereby the winter-summer temperature difference increased by up to 5.7°C at the Allerød-YD transition.

Thermal modelling shows that a thin winter snowpack effectively shielding the subsurface during the cold winters is needed to account for CCC formation commencing at 12.6 ±0.2 ka at Cioccherloch. Studies in modern permafrost areas suggest that a stable winter snow cover of only ~35 cm results in a positive shift of up to 5.5°C in the mean annual ground surface temperature (Zhang, 2005). Changes in the timing, duration, thickness and density of the snow cover may promote either the development or the degradation of permafrost (Zhang, 2005). A snowpack in the cold season leads to a positive temperature anomaly in the ground, whereas a summer snow cover insulates the ground from warm air and facilitates the development of permafrost. In a study of Arctic permafrost, Park et al. (2014) found that the thermal state of the underlying soil is more affected by early winter than peak winter snowfall. Therefore, we argue for a moderately humid early YD with snowfall during fall and early winter. Although the spatial distribution of rock glaciers from one of the driest areas of the Swiss Alps suggests a 30-

https://doi.org/10.5194/cp-2020-107
Preprint. Discussion started: 25 August 2020


Climate of the Past Discussions

40% reduction in YD precipitation compared to today (Frauenfelder et al., 2001), paleoglacier records point to similar amounts but a different seasonal distribution of precipitation in the Southern Alps with respect to modern day (Kerschner et al., 2016).

5.4 Climate change during the mid-YD

High-resolution speleothem (Baldini et al., 2015; Bartolomé et al., 2015; Rossi et al., 2018) and lake records (Bakke et al., 2009; Brauer et al., 2008; Lane et al., 2013) from W and N Europe suggest a time-transgressive change in atmospheric circulation during the YD associated with a warming of parts of Europe due to a retreat of winter sea ice and a northward migration of the polar front (e.g., Baldini et al., 2015; Bartolomé et al., 2015). At Meerfelder Maar, Germany, this so-called mid-YD transition occurred at 12.24 ±0.04 ka BP (Lane et al., 2013). This timing is strikingly similar to the error-weighted mean of the CCC dates from Cioccherloch (12.19 ±0.06 ka BP), suggesting that the main phase of CCC formation at this site may have been related to climate change. Our thermal simulations provide important constraints on the type and magnitude of climate change during the mid-YD transition at this high-alpine site and suggest a mild warming by up to 1°C (MAAT) with a slight reduction in precipitation.

A change from moderately snow-rich to snow-poor autumns and early winters from the early to the late YD combined with a small atmospheric warming (scenario 3c) is consistent with the main advance of Alpine ice glaciers (Fig. 6) during the first few centuries of the YD (Baroni et al., 2017; Heiri et al., 2014b; Ivy-Ochs et al., 2009). The subsequent glacier reduction and the parallel increase in rock-glacier activity advocate less humid conditions towards the end of the YD and the early Holocene in the Western and Eastern Alps (Ivy-Ochs et al., 2009; Kerschner and Ivy-Ochs, 2008).

Speleothem records from the Pyrenees (Baldini et al., 2015; Bartolomé et al., 2015), Cantabrian Cordiella (Rossi et al., 2018) and the Adriatic coast (Belli et al., 2017) suggest a precipitation increase in the late YD, attributed to a strengthening of the westerlies. Precipitation-sensitive archives in the northern Alps, however, do not show evidence of a major change. Benthic ostracod $\delta^{18}O$ records from Lake Ammersee (Grafenstein et al., 1999) and Lake Mondsee (Lauterbach et al., 2011) only show a gradual ca. 1‰ increase across the YD, arguing against a major step-wise change in the precipitation regime as would be expected as a result of the migration of the polar front across the Alps (Fig. 6). This slight increase in $\delta^{18}O$ values, however, is compatible with our interpretation of a small decrease in autumn precipitation in the northern alpine catchment areas of these lakes in the second half of the YD (Fig. 6) coupled with a minor (≤1°C) warming. Speleothem $\delta^{18}O$ data from Hölloch cave west of the Ammersee catchment (Wurth et al., 2004) and from the Jura Mountains (Affolter et al., 2019) likewise lack isotopic evidence of a significant change in climate within the YD. While our data and paleoglacier evidence are consistent with a slight warming at the mid-YD transition, they argue for a reduction in fall and winter precipitation. This suggests that the popular model of a south-north migration of the polar front and a concomitant increase in westerly-driven precipitation (e.g., Lane et al., 2013) is too simplistic at least for the greater Alpine realm, underscoring the need for regionally resolved climate models. In fact, even at the key site of Meerfelder Maar, the proposed increase in (winter) precipitation is poorly captured by most proxy data except for the abundance of Ti, which is attributed to spring snow melt (Lane et al., 2013).

https://doi.org/10.5194/cp-2020-107
Preprint. Discussion started: 25 August 2020

6 Conclusions

This article presents the first record of CCC in the Dolomites which formed, in contrast to many studies from Central European caves, not during a major climate warming but within a prominent stadial. These deposits indicate sustained conditions of ~0°C between ~12.6 and ~12.2 ka BP at about 50 m below the surface, initiating the slow freezing of dripwater-induced meltwater pockets in perennial cave ice. Combined with a thermal model the high-elevation setting of this cave suggests a ≤5°C drop in MAAT compared to today, incompatible with extreme winter cooling during the YD. CCC formation during the early YD requires autumn to early winter snowfall forming a sufficiently thick and stable snow cover insulating the ground from the winter cold. CCC formation during the early YD coincided with the maximum YD extent of Southern Alpine glaciers, consistent with abundant snowfall in autumn and winter and with decreased summer temperatures. Using a 0.3-4°C cooling for the short and mild early YD summers as suggested by data-model comparison studies (Heiri et al., 2014b; Schenk et al., 2018), mean January air temperatures at this alpine site were most likely not colder than -13.7°C. Seasonal temperature differences between early YD summers and winters were therefore up to 5.7°C larger than during the Allerød.

The ^{230}Th data provide strong evidence that CCC formation at ~12.2 ka occurred in response to climate change associated with the mid-YD transition. CCC formation at this high-alpine cave advocates a mild atmospheric warming (i.e. +1°C in MAAT) and a reduction in fall precipitation in the late YD. We propose a shift from snow-rich early YD towards snow-poor late YD autumns and early winters, which is consistent with the retreat of YD glaciers in the Alps and an increase in rock glacier activity.

CCCs are a novel paleoclimate archive allowing to precisely constrain permafrost thawing events in the past. Our study demonstrates that CCCs can also provide quantitative constraints on paleotemperature and seasonally resolved precipitation changes.

Code and data availability

The code for the 1d heat-flow model is available online (https://zenodo.org/record/3982221). Data is included in Tables 1 and 2 and additionally given in Supplementary Table 1.

Acknowledgements

Field work and sampling was carried out in cooperation with the Naturpark Fanes-Sennes-Prags under a permit issued by the Amt für Naturparke, Abt. 28. Natur, Landschaft und Raumentwicklung of the Autonome Provinz Bozen – Südtirol. Gottfried Nagler, Andreas Treyer and Charlotte Honiat provided support during fieldwork and Jia Xue measured two ^{230}Th ages. The Hydrographische Amt of the Autonome Provinz Bozen – Südtirol kindly provided meteorological data. Paolo Mietto is acknowledged for sharing information on the caves explored by the speleo club Proteo, Alexander Jarosch, Jeffrey S. Munroe, Yuri Dublyansky Hanns Kerschner and Paul Töchterle for fruitful discussions that helped to improve the manuscript. Stéphane

https://doi.org/10.5194/cp-2020-107
Preprint. Discussion started: 25 August 2020

375 Affolter is thanked for providing data from Milandre cave. This work was supported by the Autonome Provinz Bozen – Südtirol, Amt für Wissenschaft und Forschung (grant 3/34 to C.S.) and the Tiroler Wissenschaftsförderung grant WF-F.16947/5-2019 (to G.K.).

Author contribution

G.K. and C.S. designed the study, carried out field work, performed petrographic, stable isotope analyses and heat-flow
380 modelling. G.K. carried out uranium-series dating, supervised by H.C. G.K. wrote the paper with contributions from all co-authors.

Competing interests

The authors declare that they have no conflict of interest.

References

385 Affolter, S., Häuselmann, A., Fleitmann, D., Edwards, R. L., Cheng, H. and Leuenberger, M.: Central Europe temperature constrained by speleothem fluid inclusion water isotopes over the past 14,000 years, Sci. Adv., 5(6), eaav3809, doi:10.1126/sciadv.aav3809, 2019.

Alley, R. B.: The Younger Dryas cold interval as viewed from central Greenland, Quat. Sci. Rev., 19(1–5), 213–226, doi:10.1016/S0277-3791(99)00062-1, 2000.

390 Bakke, J., Lie, Ø., Heegaard, E., Dokken, T., Haug, G. H., Birks, H. H., Dulski, P. and Nilsen, T.: Rapid oceanic and atmospheric changes during the Younger Dryas cold period, Nat. Geosci., 2(3), 202–205, doi:10.1038/ngeo439, 2009.

Baldini, J. U. L., Brown, R. J. and Mawdsley, N.: Evaluating the link between the sulfur-rich Laacher See volcanic eruption and the Younger Dryas climate anomaly, Clim. Past, 14(7), 969–990, doi:10.5194/cp-14-969-2018, 2018.

Baldini, L. M., McDermott, F., Baldini, J. U. L., Arias, P., Cueto, M., Fairchild, I. J., Hoffmann, D. L., Mattey, D. P., Müller,
395 W., Nita, D. C., Ontañón, R., Garciá-Moncó, C. and Richards, D. A.: Regional temperature, atmospheric circulation, and sea-ice variability within the Younger Dryas Event constrained using a speleothem from northern Iberia, Earth Planet. Sci. Lett., 419, 101–110, doi:10.1016/j.epsl.2015.03.015, 2015.

Baroni, C., Casale, S., Salvatore, M. C., Ivy-Ochs, S., Christl, M., Carturan, L., Seppi, R. and Carton, A.: Double response of glaciers in the Upper Peio Valley (Rhaetian Alps, Italy) to the Younger Dryas climatic deterioration, Boreas, 46(4), 783–798,
400 doi:10.1111/bor.12284, 2017.

Bartolomé, M., Moreno, A., Sancho, C., Stoll, H. M., Cacho, I., Spötl, C., Belmonte, Á., Edwards, R. L., Cheng, H. and Hellstrom, J. C.: Hydrological change in Southern Europe responding to increasing North Atlantic overturning during

https://doi.org/10.5194/cp-2020-107
Preprint. Discussion started: 25 August 2020

Greenland Stadial 1, Proc. Natl. Acad. Sci., 112(21), 6568–6572, doi:10.1073/pnas.1503990112, 2015.

Belli, R., Borsato, A., Frisia, S., Drysdale, R., Maas, R. and Greig, A.: Investigating the hydrological significance of stalagmite geochemistry (Mg, Sr) using Sr isotope and particulate element records across the Late Glacial-to-Holocene transition, Geochim. Cosmochim. Acta, 199, 247–263, doi:10.1016/j.gca.2016.10.024, 2017.

Brauer, A., Haug, G. H., Dulski, P., Sigman, D. M. and Negendank, J. F. W.: An abrupt wind shift in western Europe at the onset of the Younger Dryas cold period, Nat. Geosci., 1(8), 520–523, doi:10.1038/ngeo263, 2008.

Broecker, W. S.: Abrupt Climate Change Revisited, Glob. Planet. Change, 56, 211–215, doi:10.1029/2011GM001139, 2006.

Broecker, W. S., Kennett, J. P., Flower, B. P., Teller, J. T., Trumbore, S., Bonani, G. and Wolfli, W.: Routing of meltwater from the Laurentide Ice Sheet during the Younger Dryas cold episode, Nature, 341(6240), 318–321, doi:10.1038/341318a0, 1989.

Broecker, W. S., Denton, G. H., Edwards, R. L., Cheng, H., Alley, R. B. and Putnam, A. E.: Putting the Younger Dryas cold event into context, Quat. Sci. Rev., 29(9–10), 1078–1081, doi:10.1016/j.quascirev.2010.02.019, 2010.

Cheng, H., Lawrence Edwards, R., Shen, C.-C., Polyak, V. J., Asmerom, Y., Woodhead, J., Hellstrom, J., Wang, Y., Kong, X., Spötl, C., Wang, X. and Calvin Alexander, E.: Improvements in ^{230}Th dating, ^{230}Th and ^{234}U half-life values, and U–Th isotopic measurements by multi-collector inductively coupled plasma mass spectrometry, Earth Planet. Sci. Lett., 371–372, 82–91, doi:https://doi.org/10.1016/j.epsl.2013.04.006, 2013.

Edwards, R. L., Chen, J. H. and Wasserburg, G. J.: 238U234U230Th232Th systematics and the precise measurement of time over the past 500,000 years, Earth Planet. Sci. Lett., 81(2), 175–192, doi:https://doi.org/10.1016/0012-821X(87)90154-3, 1987.

Frauenfelder, R., Haeberli, W., Hoelzle, M. and Maisch, M.: Using relict rockglaciers in GIS-based modelling to reconstruct Younger Dryas permafrost distribution patterns in the Err-Julier area, Swiss Alps, Nor. Geogr. Tidsskr., 55(4), 195–202, doi:10.1080/00291950152746522, 2001.

Ghadiri, E., Vogel, N., Brennwald, M. S., Maden, C., Häuselmann, A. D., Fleitmann, D., Cheng, H. and Kipfer, R.: Noble gas based temperature reconstruction on a Swiss stalagmite from the last glacial–interglacial transition and its comparison with other climate records, Earth Planet. Sci. Lett., 495, 192–201, doi:10.1016/j.epsl.2018.05.019, 2018.

Grafenstein, U. Von, Erlenkeuser, H., Brauer, A., Jouzel, J., Johnsen, S. J. and von Grafenstein, U.: A Mid-European Decadal Isotope-Climate Record from 15,500 to 5000 Years B.P., Science (80-.)., 1654(1999), 1654–1657, doi:10.1126/science.284.5420.1654, 1999.

Von Grafenstein, U., Eicher, U., Erlenkeuser, H., Ruch, P., Schwander, J. and Ammann, B.: Isotope signature of the Younger Dryas and two minor oscillations at Gerzensee (Switzerland): Palaeoclimatic and palaeolimnologic interpretation based on bulk and biogenic carbonates, Palaeogeogr. Palaeoclimatol. Palaeoecol., 159(3–4), 215–229, doi:10.1016/S0031-0182(00)00086-9, 2000.

Hanley, E. J., Dewitt, D. P. and Roy, R. F.: The thermal diffusivity of eight well-characterized rocks for the temperature range 300–1000 K, Eng. Geol., 12, 31–47, doi:https://doi.org/10.1016/0013-7952(78)90003-0, 1978.

https://doi.org/10.5194/cp-2020-107
Preprint. Discussion started: 25 August 2020

Heiri, O., Koinig, K. A., Spötl, C., Barrett, S., Brauer, A., Drescher-Schneider, R., Gaar, D., Ivy-Ochs, S., Kerschner, H., Luetscher, M., Moran, A., Nicolussi, K., Preusser, F., Schmidt, R., Schoeneich, P., Schwörer, C., Sprafke, T., Terhorst, B. and Tinner, W.: Palaeoclimate records 60–8 ka in the Austrian and Swiss Alps and their forelands, Quat. Sci. Rev., 106, 186–205, doi:https://doi.org/10.1016/j.quascirev.2014.05.021, 2014a.

Heiri, O., Brooks, S. J., Renssen, H., Bedford, A., Hazekamp, M., Ilyashuk, B., Jeffers, E. S., Lang, B., Kirilova, E., Kuiper, S., Millet, L., Samartin, S., Toth, M., Verbruggen, F., Watson, J. E., van Asch, N., Lammertsma, E., Amon, L., Birks, H. H., Birks, H. J. B., Mortensen, M. F., Hoek, W. Z., Magyari, E., Muñoz Sobrino, C., Seppä, H., Tinner, W., Tonkov, S., Veski, S. and Lotter, A. F.: Validation of climate model-inferred regional temperature change for late-glacial Europe, Nat. Commun., 5, 4914, doi:10.1038/ncomms5914, 2014b.

Hepp, J., Wüthrich, L., Bromm, T., Bliedtner, M., Schäfer, I. K., Glaser, B., Rozanski, K., Sirocko, F., Zech, R. and Zech, M.: How dry was the Younger Dryas? Evidence from a coupled δ^2H and $\delta^{18}O$ biomarker paleohygrometer applied to the Gemündener Maar sediments, Western Eifel, Germany, Clim. Past, 15(2), 713–733, doi:10.5194/cp-15-713-2019, 2019.

Ivy-Ochs, S., Kerschner, H., Maisch, M., Christl, M., Kubik, P. W. and Schlüchter, C.: Latest Pleistocene and Holocene glacier variations in the European Alps, Quat. Sci. Rev., 28(21–22), 2137–2149, doi:10.1016/j.quascirev.2009.03.009, 2009.

Kerschner, H. and Ivy-Ochs, S.: Palaeoclimate from glaciers: Examples from the Eastern Alps during the Alpine Lateglacial and early Holocene, Glob. Planet. Change, 60(1–2), 58–71, doi:10.1016/j.gloplacha.2006.07.034, 2008.

Kerschner, H., Kaser, G. and Sailer, R.: Alpine Younger Dryas glaciers as palaeo-precipitation gauges, Ann. Glaciol., 31(August 1999), 80–84, 2000.

Kerschner, H., Moran, A. and Ivy-Ochs, S.: Younger Dryas equilibrium line altitudes and precipitation patterns in the Alps, Geophys. Res. Abstr., 18(2000), 1 [online] Available from: https://meetingorganizer.copernicus.org/EGU2016/posters/21136, 2016.

Lane, C. S., Brauer, A., Blockley, S. P. E. and Dulski, P.: Volcanic ash reveals time-transgressive abrupt climate change during the Younger Dryas, Geology, 41(12), 1251–1254, doi:10.1130/G34867.1, 2013.

Lauterbach, S., Brauer, A., Andersen, N., Danielopol, D. L., Dulski, P., Hüls, M., Milecka, K., Namiotko, T., Obremska, M. and Von Grafenstein, U.: Environmental responses to Lateglacial climatic fluctuations recorded in the sediments of pre-Alpine Lake Mondsee (northeastern Alps), J. Quat. Sci., 26(3), 253–267, doi:10.1002/jqs.1448, 2011.

Lotter, A. F., Birks, H. J. B., Eicher, U., Hofmann, W., Schwander, J. and Wick, L.: Younger Dryas and Allerød summer temperatures at Gerzensee (Switzerland) inferred from fossil pollen and cladoceran assemblages, Palaeogeogr. Palaeoclimatol. Palaeoecol., 159, 349–361, doi:https://doi.org/10.1016/S0031-0182(00)00093-6, 2000.

Luetscher, M., Hellstrom, J., Müller, W., Barrett, S. and Dublyansky, Y.: A Younger Dryas temperature reconstruction from alpine speleothems, Geophys. Res. Abstr., 18, 11602, 2016.

Moran, A. P., Ivy-Ochs, S., Schuh, M., Christl, M. and Kerschner, H.: Evidence of central Alpine glacier advances during the Younger Dryas–early Holocene transition period, Boreas, 45(3), 398–410, doi:10.1111/bor.12170, 2016.

Naughton, F., Costas, S., Gomes, S. D., Desprat, S., Rodrigues, T., Sanchez Goñi, M. F., Renssen, H., Trigo, R., Bronk-

https://doi.org/10.5194/cp-2020-107
Preprint. Discussion started: 25 August 2020

Ramsey, C., Oliveira, D., Salgueiro, E., Voelker, A. H. L. and Abrantes, F.: Coupled ocean and atmospheric changes during Greenland stadial 1 in southwestern Europe, Quat. Sci. Rev., 212, 108–120, doi:10.1016/j.quascirev.2019.03.033, 2019.

Oberli, F., Ilyashuk, E., van der Knaap, W. O., Lotter, A. F., Gobet, E., Heiri, O., Ammann, B., van Leeuwen, J. F. N. and Ilyashuk, B.: Lateglacial environmental and climatic changes at the Maloja Pass, Central Swiss Alps, as recorded by chironomids and pollen, Quat. Sci. Rev., 28(13–14), 1340–1353, doi:10.1016/j.quascirev.2009.01.007, 2009.

Park, H., Fedorov, A. N. and Walsh, J. E.: Effect of snow cover on pan-Arctic permafrost thermal regimes, Clim. Dyn., doi:10.1007/s00382-014-2356-5, 2014.

Perşoiu, A.: Chapter 3 - Ice Caves Climate, in Ice Caves, edited by A. Perşoiu and S.-E. Lauritzen, pp. 21–32, Elsevier., 2018.

Renssen, H., Lautenschlager, M. and Schuurmans, C. J. E.: The atmospheric winter circulation during the Younger Dryas stadial in the Atlantic/European sector, Clim. Dyn., 12(12), 813–824, doi:10.1007/s003820050145, 1996.

Renssen, H., Mairesse, A., Goosse, H., Mathiot, P., Heiri, O., Roche, D. M., Nisancioglu, K. H., Mairesse, A. and Valdes, P. J.: Multiple causes of the Younger Dryas cold period, Nat. Geosci., 8(12), 946–949, doi:10.1038/ngeo2557, 2015.

Richter, D. and Reichelmann, D.: Late Pleistocene cryogenic calcite spherolites from the Malachitdom Cave (NE Rhenish Slate Mountains, Germany): origin, unusual internal structure and stable C-O isotope composition, Int. J. Speleol., 37(2), 119–129, doi:10.5038/1827-806x.37.2.5, 2012.

Rossi, C., Bajo, P., Lozano, R. P. and Hellstrom, J.: Younger Dryas to Early Holocene paleoclimate in Cantabria (N Spain): Constraints from speleothem Mg, annual fluorescence banding and stable isotope records, Quat. Sci. Rev., 192, 71–85, doi:10.1016/j.quascirev.2018.05.025, 2018.

Šafanda, J. and Rajver, D.: Signature of the last ice age in the present subsurface temperatures in the Czech Republic and Slovenia, Glob. Planet. Change, 29(3), 241–257, doi:https://doi.org/10.1016/S0921-8181(01)00093-5, 2001.

Schenk, F., Väliranta, M., Muschitiello, F., Tarasov, L., Heikkilä, M., Björck, S., Brandefelt, J., Johansson, A. V., Näslund, J.-O. and Wohlfarth, B.: Warm summers during the Younger Dryas cold reversal, Nat. Commun., 9(1), doi:10.1038/s41467-018-04071-5, 2018.

Schlolaut, G., Brauer, A., Nakagawa, T., Lamb, H. F., Tyler, J. J., Staff, R. A., Marshall, M. H., Bronk Ramsey, C., Bryant, C. L. and Tarasov, P. E.: Evidence for a bi-partition of the Younger Dryas Stadial in East Asia associated with inversed climate characteristics compared to Europe, Sci. Rep., 7(44983), doi:10.1038/srep44983, 2017.

Spötl, C. and Cheng, H.: Holocene climate change, permafrost and cryogenic carbonate formation: Insights from a recently deglaciated, high-elevation cave in the Austrian Alps, Clim. Past, 10(4), 1349–1362, doi:10.5194/cp-10-1349-2014, 2014.

Spötl, C. and Vennemann, T. W.: Continuous-flow isotope ratio mass spectrometric analysis of carbonate minerals, Rapid Commun. Mass Spectrom., 17(9), 1004–1006, doi:doi:10.1002/rcm.1010, 2003.

Stute, M. and Deak, J.: Environmental isotope study (14C, 13C, 18O, D, noble gases) on deep groundwater circulation systems in Hungary with reference to paleoclimate, Radiocarbon, 31(3), 902–918, 1989.

Varsányi, I., Palcsu, L. and Kovács, L. Ó.: Groundwater flow system as an archive of palaeotemperature: Noble gas, radiocarbon, stable isotope and geochemical study in the Pannonian Basin, Hungary, Appl. Geochemistry, 26(1), 91–104,

505 doi:https://doi.org/10.1016/j.apgeochem.2010.11.006, 2011.

Wurth, G., Niggemann, S., Richter, D. K. and Mangini, A.: The Younger Dryas and Holocene climate record of a stalagmite from Hölloch Cave (Bavarian Alps, Germany), J. Quat. Sci., 19(3), 291–298, doi:10.1002/jqs.837, 2004.

Žák, K., Richter, D. K.Filippi, M., Živor, R., Deininger, M., Mangini, A. and Scholz, D.: Coarsely crystalline cryogenic cave carbonate – a new archive to estimate the Last Glacial minimum permafrost depth in Central Europe, Clim. Past,
510 8(6), 1821–1837, doi:10.5194/cp-8-1821-2012, 2012.

Žák, K., Onac, B. P., Kadebskaya, O. I., Filippi, M., Dublyansky, Y. and Luetscher, M.: Cryogenic Mineral Formation in Caves., 2018.

Zhang, T.: Influence of the seasonal snow cover on the ground thermal regime: an overview, Rev. Geophys., 43, RG4002, doi:10.1029/2004RG000157, 2005.

515

https://doi.org/10.5194/cp-2020-107
Preprint. Discussion started: 25 August 2020

Figures

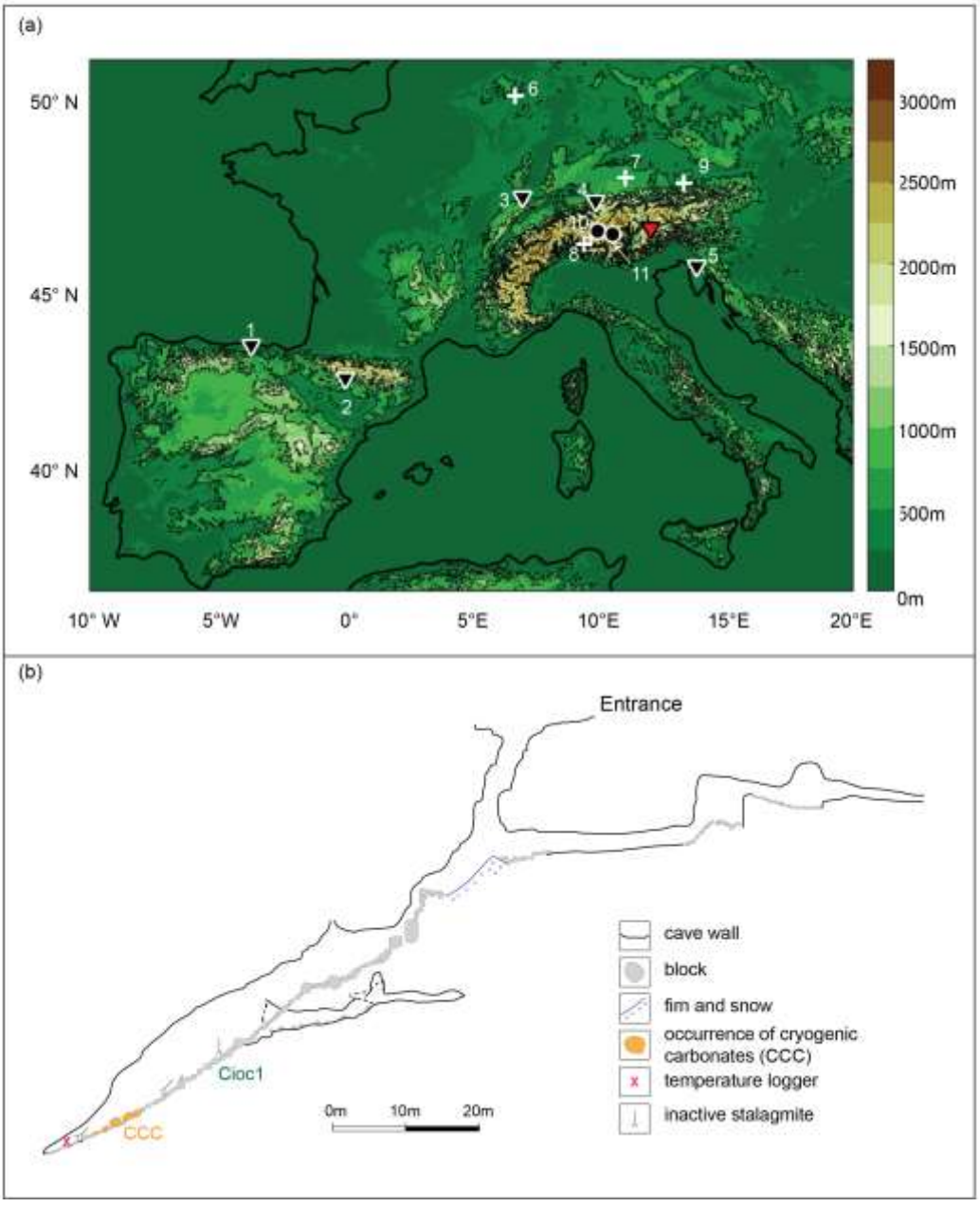

520 **Figure 1: Relief map of Europe showing the location of Cioccherloch (red triangle) and other European YD speleothem (black triangle), lacustrine (white cross) and palaeoglacier (black circle) records (a) mentioned in the text (1 −La Garma cave, 2 − Seso cave, 3 − Milandre cave, 4 −Bärenhöhle, 5 −Savi cave, 6 −Meerfelder Maar, 7 − Lake Ammmersee, 8 −Majola Pass, 9 – Mondsee 10 −Err-Julier and Julier Pass, 11 −Ortles). Vertical cross section of Cioccherloch cave showing the CCC findings in the terminal chamber (b).**

https://doi.org/10.5194/cp-2020-107
Preprint. Discussion started: 25 August 2020

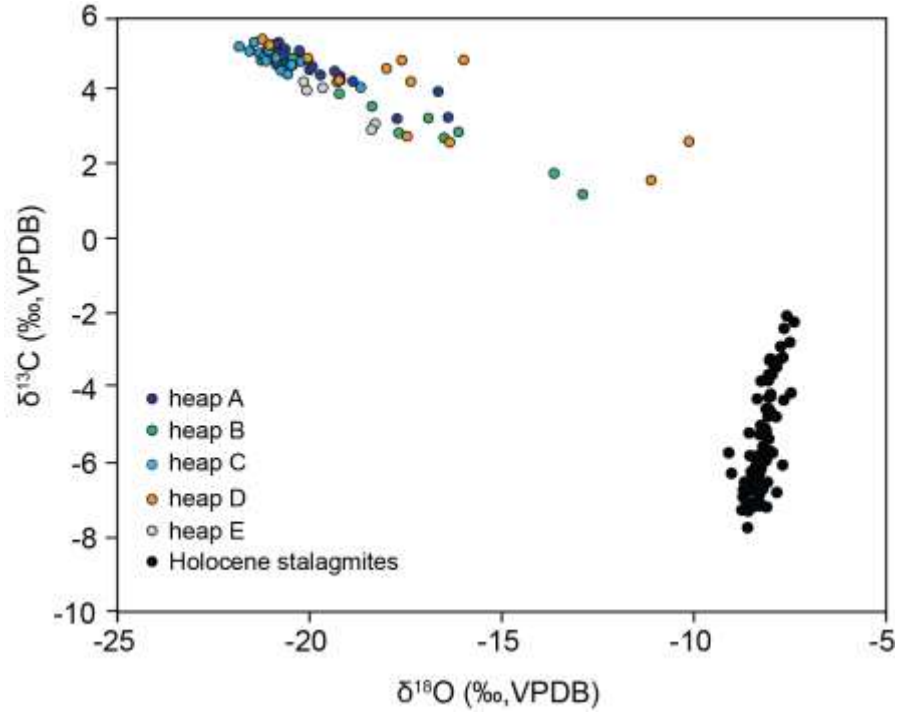

525

Figure 2: Stable isotope composition of CCCs from Cioccherloch cave. Samples from different CCC heaps are color-coded. Values of two Holocene stalagmites from the same cave gallery are shown for comparison (unpublished data by the authors).

https://doi.org/10.5194/cp-2020-107
Preprint. Discussion started: 25 August 2020

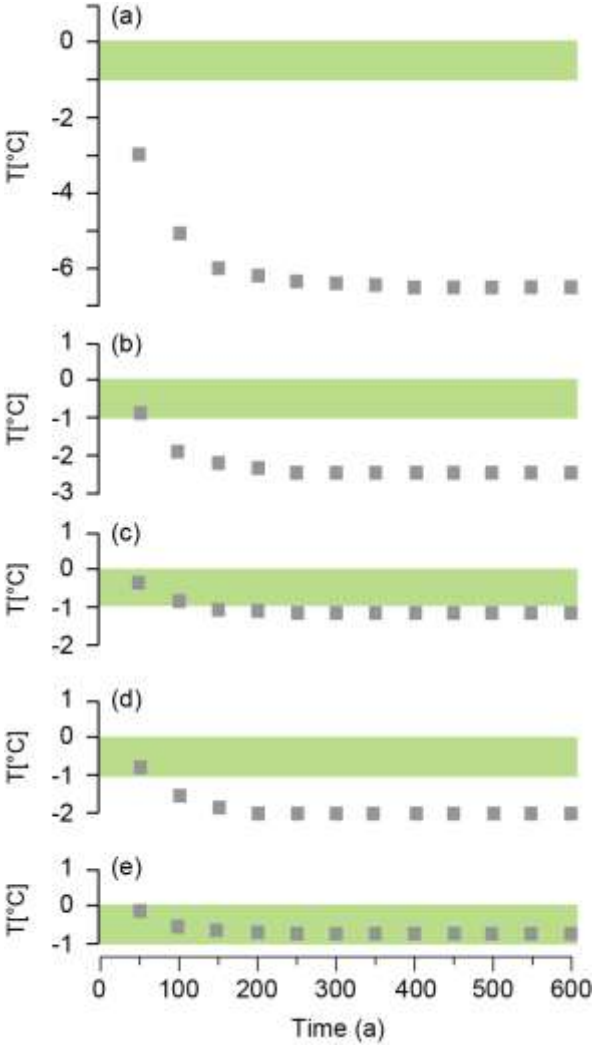

Figure 3: Thermal models 2a to 2e simulating the development and deepening of the permafrost during the early YD. Modeling results depict the ground temperature at 50 m depth at the depth of the CCC site in Cioccherloch. These models use the temperature profile of scenario 1 as initial condition. Model 2a (a) is forced with a MAAT of -6.5°C. Models 2b (b) and 2c (c) use a MAAT of -2.5°C and the latter simulates the impact of a winter snow cover resulting in the attenuation of the winter cold by 5°C (i.e. ΔT = 5°C). Scenarios 2d (d) and 2e (e) model the changes of the thermal profile at the CCC site using a MAAT of -1.5°C. Scenario 2e considers the presence of a winter snow pack resulting in ΔT of 4.5°C. The green horizontal bar marks the -1 to 0°C "window" of possible CCC formation for the depth range of the CCC site in this cave.

https://doi.org/10.5194/cp-2020-107
Preprint. Discussion started: 25 August 2020

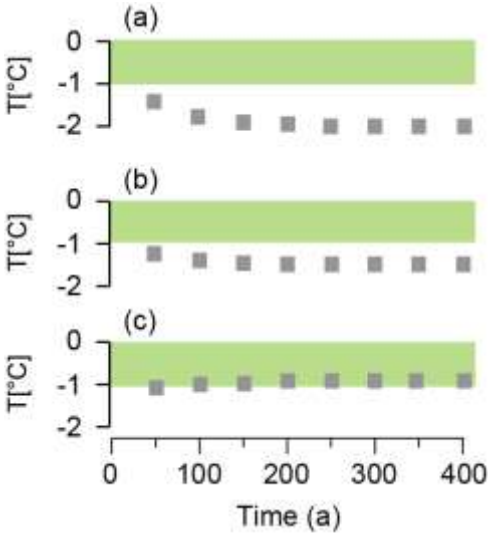

Figure 4: Thermal model runs simulating a change in YD climate starting at 12.24 ka (mid-YD transition). Results show the ground temperature at 50 m depth (grey rectangles), at the depth of the CCC site in Cioccherloch. Model 3a (a) simulates the subsurface thermal conditions for a MAAT identical to scenario 2e (i.e. MAAT -2.0°C) but the autumns and winters became drier resulting in a reduction of the winter snow cover (ΔT=2.0°C). Scenarios 3b (b) and 3c (c) simulate the impact of a +1°C rise in MAAT with respect to scenario 2c (i.e. MAAT -1.5°C) and the 3c model also includes a thin winter snow cover (ΔT=2.5°C). The green horizontal bar marks the -1 to 0 °C "window" of possible CCC formation at the depth of the CCC site in Cioccherloch.

https://doi.org/10.5194/cp-2020-107
Preprint. Discussion started: 25 August 2020

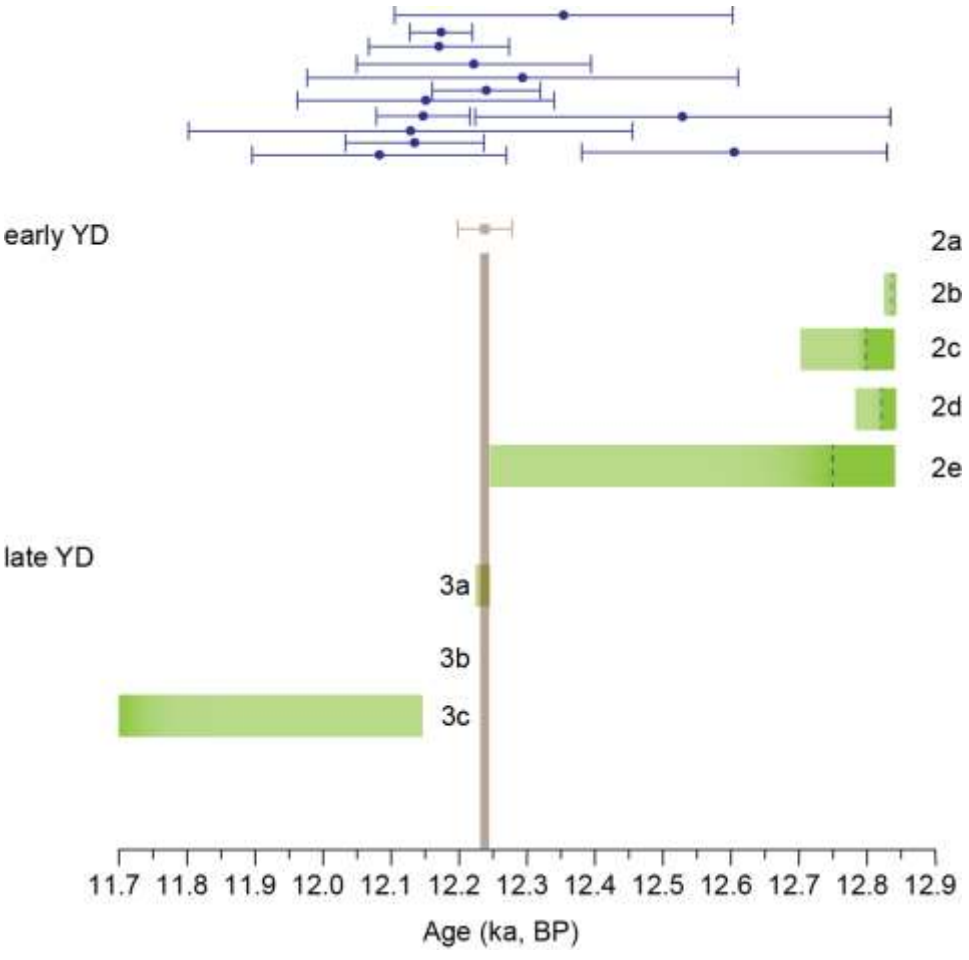

Figure 5: ^{230}Th ages of CCC and their 2σ uncertainties from Cioccherloch (blue bars) and CCC formation "windows" as suggested by model scenarios for the early and late YD. The green bars mark the -1 to 0°C window of possible CCC formation at the depth of the CCC site. The blue dashed vertical lines mark the -0.5°C isotherm at 50 m depth (2c-2e). The brown vertical line and age with the 2σ error bar mark the timing of the mid-YD transition at Meerfelder Maar (Lane et al., 2013).

https://doi.org/10.5194/cp-2020-107
Preprint. Discussion started: 25 August 2020

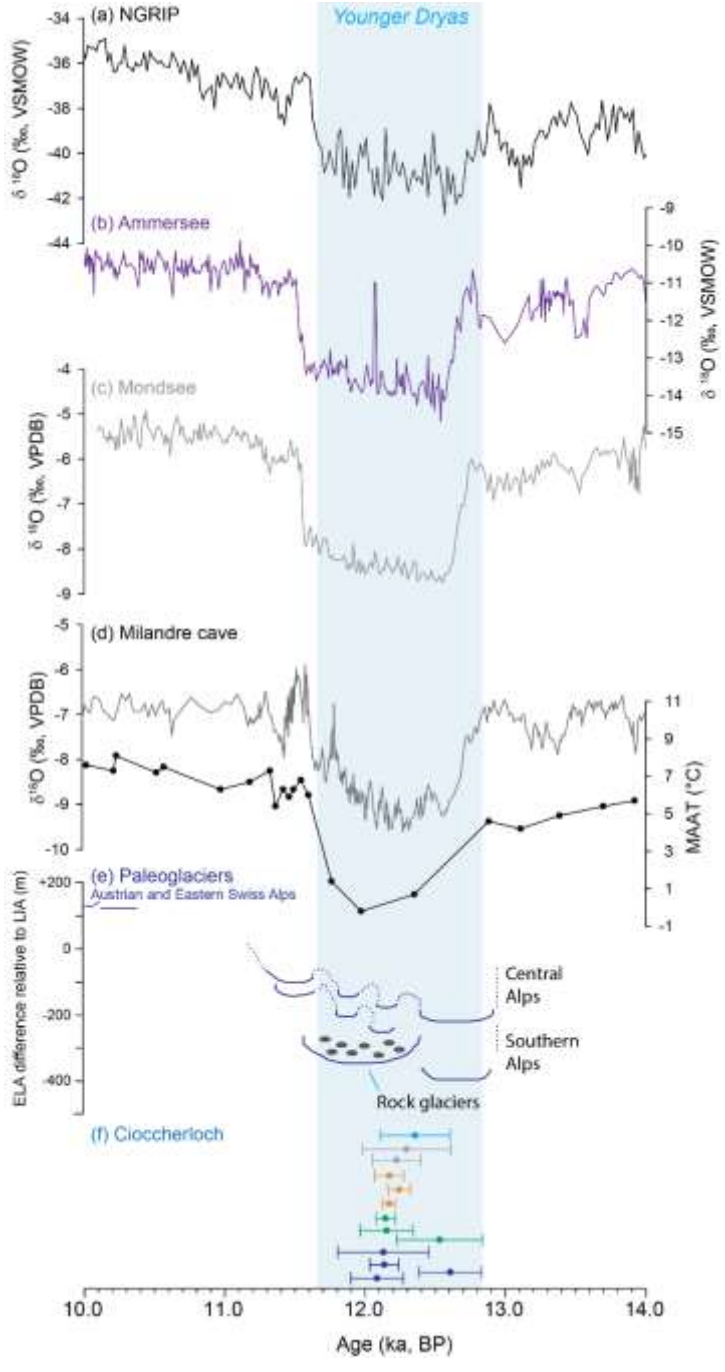

Figure 6: CCC ages from Cioccherloch (f) compared to YD proxy records in Europe and Greenland plotted on their published chronology. (a) NGRIP $\delta^{18}O$ data (Rasmussen et al., 2014), (b) lacustrine benthic ostracod $\delta^{18}O$ data from Ammersee (von Grafenstein et al., 1999) and (c) Mondsee (Lauterbach et al., 2011), (d) speleothem $\delta^{18}O$ data and MAAT inferred from fluid inclusion stable isotope data of stalagmites from Milandre cave (Affolter et al., 2019), and (e) extent of Central and Southern Alpine paleoglaciers (Heiri et al., 2014b). Dark blue and green refer to ^{230}Th ages of CCCs from heap A and B, respectively (f). Data from heaps C, D and E are shown in orange, grey and light blue, respectively (f).

https://doi.org/10.5194/cp-2020-107
Preprint. Discussion started: 25 August 2020

Climate of the Past Discussions
Open Access
EGU

Tables

Table 1: ^{230}Th dating results of cryogenic calcite samples (FOS12) and a stalagmite (Cioc1) from Cioccherloch. Letters in the sample names of CCC (i.e. A, B, C, D, E) indicate the heap where the sample was collected, as shown in Fig. 2. Four samples were excluded from the discussion (italics) because of their excessive ^{232}Th values. $\delta^{234}U = ([^{234}U/^{238}U]_{activity} - 1)x1000$. $\delta^{234}U_{initial}$ was calculated based on ^{230}Th age (t). i.e. $\delta^{234}U_{initial} = \delta^{234}U_{measured} \times e^{\lambda 234 \times t}$. Ages are reported as BP. i.e. before the year 1950 AD. The error is 2 sigma.

Sample	^{238}U (ppb)	^{232}Th (ppt)	^{230}Th/^{232}Th (atomicx10^{-6})	$\delta^{234}U$ (measured)	^{230}Th/^{238}U (activity)	^{230}Th age (ka) (uncorr.)	$\delta^{234}U_{initial}$ (corr.)	230Th age (ka) (corr.)
FOS12-A10	1883 ± 2	18024 ± 361	208 ± 4	121.9 ± 1.3	0.1208 ± 0.0006	12.40 ± 0.07	126 ± 1	12.08 ± 0.19
FOS12-A12	*1139 ± 2*	*53468 ± 1074*	*46 ± 1*	*124.8 ± 2.2*	*0.1303 ± 0.0007*	*13.40 ± 0.08*	*129 ± 2*	*12.11 ± 0.86*
FOS12-A3a	*1863 ± 3*	*41219 ± 828*	*93 ± 2*	*125.0 ± 2.1*	*0.1252 ± 0.0006*	*12.83 ± 0.07*	*129 ± 2*	*12.20 ± 0.41*
FOS12-A3b	1810 ± 3	20310 ± 408	185 ± 4	123.0 ± 2.1	0.1261 ± 0.0008	12.96 ± 0.09	128 ± 2	12.60 ± 0.22
FOS12-A1	1480 ± 9	934 ± 21	3113 ± 70	121.4 ± 2.9	0.1191 ± 0.0009	12.22 ± 0.10	126 ± 3	12.13 ± 0.10
FOS12-A2	1893 ± 19	29808 ± 666	128 ± 3	120.5 ± 4.4	0.1225 ± 0.0014	12.60 ± 0.16	125 ± 5	12.13 ± 0.33
FOS12-B4	1492 ± 3	24543 ± 493	127 ± 3	124.0 ± 2.1	0.1268 ± 0.0004	13.02 ± 0.05	128 ± 2	12.53 ± 0.31
FOS12-B5	*1790 ± 4*	*77634 ± 1564*	*53 ± 1*	*121.8 ±2.5*	*0.1382 ± 0.0006*	*14.30 ± 0.08*	*126 ± 3*	*13.11 ± 0.80*
FOS12-B6	1978 ± 2	6288 ± 126	622 ±13	122.4 ±1.4	0.1199 ± 0.0003	12.30 ± 0.04	127 ± 1	12.15 ± 0.07
FOS12-B10	2095 ± 4	19878 ± 339	211 ± 4	121.1 ± 2.1	0.1213 ± 0.0006	12.47 ± 0.07	125 ± 2	12.15 ± 0.19
FOS12-C	1979 ± 4	25984 ± 522	156 ± 3	123.1 ± 2.0	0.1243 ± 0.0006	12.76 ± 0.06	127 ± 2	12.35 ± 0.25
FOS12-D	1782 ± 1	6916 ± 139	514 ± 10	122.8 ± 1.3	0.1210 ± 0.0003	12.41 ± 0.04	127 ± 1	12.24 ± 0.08
FOS12-D3	*1458 ± 3*	*47447 ± 953*	*61 ± 1*	*121.9 ± 2.0*	*0.1212 ± 0.0005*	*12.44 ± 0.06*	*126 ± 2*	*11.53 ± 0.60*
FOS12-D9	2189 ± 2	3975 ± 80	1087 ± 22	121.4 ±1.4	0.1197 ± 0.0003	12.29 ± 0.03	126 ± 1	12.17 ± 0.05
FOS12-D10	1760 ± 2	8134 ± 160	430 ± 9	123.4 ± 1.6	0.1206 ± 0.0005	12.36 ± 0.06	128 ± 2	12.17 ± 0.10
FOS12-E	826 ± 1	6841 ± 137	242 ± 5	121.5 ± 1.3	0.1217 ± 0.0007	12.50 ± 0.08	126 ± 1	12.22 ± 0.17
FOS12-E2	2026 ± 3	34463 ± 693	121 ± 2	121.2 ± 1.9	0.1244 ± 0.0005	12.80 ± 0.06	126 ± 2	12.29 ± 0.32
Cioc1-1	47 ± 0.1	396 ± 8	34 ± 5	177.4 ± 3.3	0.0171 ± 0.0024	1.59 ± 0.23	178 ± 3	1.32 ± 0.27
Cioc1-2	47 ± 0.1	293 ± 6	175 ± 5	200.1 ± 2.8	0.0654 ± 0.0012	6.10 ± 0.11	203 ± 3	5.88 ± 0.15
Cioc1-3	46 ± 0.1	80 ± 2	1570 ± 36	273.1 ± 2.3	0.1653 ± 0.0014	15.09 ± 0.14	285 ± 2	14.98 ± 0.14

https://doi.org/10.5194/cp-2020-107
Preprint. Discussion started: 25 August 2020

Climate of the Past Discussions
Open Access
EGU

Table 2: Input parameters for 1d heat conduction models simulating climate during the Allerød interstadial (1), the early YD (2a-2e) and the late YD at the study site (3a-3c). Snow ΔT ascribes the attenuation of the winter cold by the snowpack, whereas the resultant annual air temperature used as a boundary condition for the thermal model is described as mean the annual effective temperature (MAET). Modern day values are shown for comparison.

	Modern	**Allerød**	**Early YD**					**Late YD**		
		Scenario 1	**Scenario 2a**	**Scenario 2b**	**Scenario 2c**	**Scenario 2d**	**Scenario 2e**	**Scenario 3a**	**Scenario 3b**	**Scenario 3c**
T July [°C]	11	9	7	8	8	8	8	8	8	8
T January [°C]	-6	-8	-20	-13	-13	-12	-12	-12	-11	-11
MAAT [°C]	2.5	0.5	-6.5	-2.5	-2.5	-2.0	-2.0	-2.0	-1.5	-1.5
Snow ΔT [°C]		-	-	-	5	-	4.7	-	-	2.5
MAET [°]		-	-	-	-1.3	-	-0.9	-	-	-0.8
Initial thermal conditions		-	output of scenario 1	output of scenario 1	output of scenario 1	output of scenario1	output of scenario 1	output of scenario 2e	output of scenario 2c	output of scenario 2c